iomac
International Operational Modal Analysis Conference

11th International Operational Modal Analysis Conference

20 - 23 May 2025 | Rennes, France

Detection of Stall Induced Vibrations in Standstill Wind Turbines

Chandramouli Santhanam [1], *Torben Knudsen*[1] *and David John Laino* [2]

[1] Department of Electronic Systems, Aalborg University, Fredrik Bajers Vej 7, 9220 Aalborg Øst, Denmark, tk@es.aau.dk
[2] Vestas Wind Systems A/S, Hedeager 42, 8200 Aarhus N, Denmark, dadla@vestas.com

ABSTRACT
Under specific inflow conditions, wind turbines in parked conditions with blades pitched to full feather (90°) can experience Stall-Induced Vibrations (SIV), leading to significant edgewise blade loads and potential blade failure. To enhance safety during standstill and enable control actions, detecting SIV is crucial. In this study, two detection methods are explored: (1) Monitoring of edgewise vibration peaks and (2) a Multi-Model (MM) state estimation approach. The peak monitoring method establishes baseline vibration peak levels and identifies deviations from these normal levels, offering a straightforward approach for early detection. The MM estimator method, in contrast, relies on a dynamic model of the vibrating blade that accounts for both lightly damped linear oscillations as well as non-linear SIV in which the vibrations grow and sustain into a limit cycle. The model, derived from a differential equation describing turbine blade vibrations, incorporates a forcing term parameterized by wind speed, yaw angle, and other parameters to switch between linear and nonlinear behaviors. The model is extended to a stochastic differential equation to include turbulent wind inflow. A Multi Model (MM) estimator based on the Interacting Multiple Model method is used to estimate states and parameters of the system. Once the parameters are estimated, SIV is detected based on the estimated coefficients. The models are evaluated on blade load data obtained from a measurement campaign on a standstill wind turbine. The results show that both the methods capture the presence of strong vibrations well. While simpler methods like the peak monitoring method might sometimes enable a quicker detection of SIV, they are prone to false alarms. Model based detection methods, like the MM estimator method might have a slightly delayed detection but can also provide information about the decreasing trend of vibrations, which can be useful in devising control strategies.

Keywords: Fault detection ; Condition Monitoring ; Stall Induced Vibrations ; Multi Model State estimation ; Non linear dynamics

1. INTRODUCTION

Under inflow conditions where the inflow yaw angle is around the stall angle range of wind turbine blade airfoils (defined in this work as between 15° - 40°), wind turbines in parked conditions can experience dangerous fluid-induced vibrations due to negative aerodynamic damping [1, 2]. These vibrations, called Stall Induced Vibrations (SIV) can lead to large blade loads in the edgewise direction. Frequent occurrences of SIV can lead to fatigue life reduction and ultimately even cause blade failure [3]. With wind turbine blades getting longer and hence more flexible, there is an imperative need to protect the turbine from serious occurrences of SIV by devising suitable detection methods. The significance of this problem within the industry is highlighted by the participation of leading wind energy companies in the PRESTIGE project [4], a dedicated three-year initiative aimed at investigating the stability of wind turbines in standstill conditions. Further evidence of the industry's commitment to addressing the SIV problem is seen from the patents filed by major companies for detecting and mitigating such vibrations [5, 6].

SIV can be detected by monitoring the edgewise vibrations of the blade and flagging anomalies. One class of methods that are commonly used to flag anomalies from the vibration signals are time-domain methods which analyze vibration signals using statistical metrics such as peak values, root mean square, and crest factor [7] of the signal. In this approach, vibration data under normal conditions is used to establish a baseline for the chosen metric. Subsequently, real-time vibration data is continuously monitored, and deviations from the baseline are analyzed. The advantage of such methods is that they are simple to implement without requiring any transformation or model development. However, these methods suffer from non-robustness associated with determining the baseline, and difficulty in differentiating faults from vibrations due to turbulence. Other class of methods are frequency-domain based methods which are mainly based on the spectrogram of the vibrations. These methods are plenty in literature and practice in comparison to time-domain methods as they give insights into the nature of faults as well.

Another class of methods that have been less focused on are model based methods which employ a model of the wind turbine and use techniques such as a Kalman Filter to estimate the states of the system. A standstill wind turbine can exhibit both stable and unstable behaviours based on the inflow yaw angle [8]. Hence, if the inflow conditions change with time, the behaviour of the turbine also changes. Multi Model (MM) estimators can be used to estimate states and parameters in such time-varying systems [9]. In the context of wind energy, MM estimators have been sparingly used. [10] developed an MM estimator for state estimation in a hydraulic wind power system, while [11] used MM estimators to estimate the effective wind speed. To the best of the authors' knowledge, MM estimators have not been used for other applications related to wind turbines, especially related to condition monitoring.

In this study, we discuss two approaches to detect SIV with one based on the peak monitoring method, and another based on MM state estimation. The novel contribution of this study is two fold. First, such an analysis of detection of SIV has not been attempted in academic literature and this study is a new contribution to this field. Secondly, the use of MM estimators in anomaly detection in wind turbines has not been attempted, and this study is a new contribution.

2. DETECTION METHODS

2.1. Peak monitoring method

In this study, a time domain method based on monitoring the peaks of the response is developed which also serves as a reference to evaluate the performance of the MM estimator. The peak values of vibration are chosen as the metric to be evaluated in the time domain. Usage of the peak to peak amplitude, which is a very similar metric is also of interest in the wind energy industry to detect and control excessive standstill vibrations [12].

In the past, few studies have focused on fault detection methods based on peak monitoring in operating

wind turbines, for example [13] in which the authors showed that the vibration peaks can be modeled using an Extreme Value distribution, and showed that the distribution parameters vary significantly during normal behaviour and faulty behaviour. However, [13] does not discuss the threshold of the deviation or provide a metric that could be used to decide when to declare a fault. In this work, a similar approach using the distribution of the peaks is developed to detect severe vibrations. However, apart from just analyzing the distributions while monitoring, the probability of fault (SIV), is also calculated. The steps involved are:

1. Vibration data under normal conditions (No SIV) is collected and the peaks are extracted. A Generalized Extreme Value (GEV) distribution is then fitted to the peak data. Let f_N and F_N denote the Probability Density Function (PDF) and Cumulative Distribution Function (CDF) of this distribution.

2. In real time, the monitoring of SIV is performed every L seconds. Let t_o denote the time instant of the start of the monitoring window, and Δt denote the sampling interval. Then, the vibration data $y_L = \{y(t_o), y(t_o + \Delta t), ...y(t_o + L)\}$, is collected and the peaks $\mathcal{P}_L$ of y_L are extracted. A GEV distribution is fitted to $\mathcal{P}_L$.

3. The goodness of fit of the distribution is analyzed using hypothesis testing. The null hypothesis is that there is no evidence to conclude that $\mathcal{P}_L$ does not follow a GEV distribution. The Anderson-Darling test (AD test) is used to calculate the p value of the hypothesis, and a significance level of 5% is chosen for the test. If $p \geq 0.05$, the null hypothesis is accepted.

   If $p < 0.05$, the null hypothesis is rejected and the distribution fitted to $\mathcal{P}_L$ is disregarded. Then, a window of length $2L$, $y_{2L} = \{y(t_o), y(t_o + \Delta t), ...y(t_o + 2L)\}$ is formed by concatenating a new window to y_L. Similarly, the peaks $\mathcal{P}_{2L}$ are extracted and a GEV is fitted to $\mathcal{P}_{2L}$, and the hypothesis testing is performed. This process is repeated until the null hypothesis is accepted. Let f_R and F_R denote the PDF and CDF of the GEV distribution fitted to the real time data.

4. The PDFs f_N and f_R are illustrated in Figure 1.

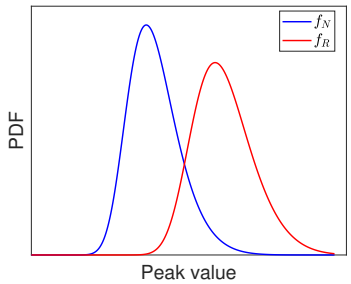

Figure 1: Illustration of the distributions f_N and f_R used to formulate probability of SIV.

Let the random variables corresponding to f_N and f_R be denoted by N and R respectively. The probability of the observed peaks in real time being less than the peaks observed in normal behaviour represents the probability of no SIV, $P_{_{safe}}$ in real time, which can be written as the joint probability $f_{NR}(n, r)$ over the domain D where the real time vibration levels are lesser than the normal vibration levels, i.e. $R \leq N$.

$$P_{_{safe}} = \int_D \int f_{NR}(n, r)\, dn\, dr \tag{1}$$

Since N and R are independent,

$$P_{_{safe}} = \int_{n=0}^{\infty} \int_{r=0}^{n} f_N(n).f_R(r)\, dr\, dn \tag{2}$$

$$P_{_{safe}} = \int_0^{\infty} F_R(x).f_N(x)dx \tag{3}$$

(3) is similar to the definition of probability of failure in structural reliability analysis considering the distributions of material strength and load [14]. The probability of SIV, P_{SIV} is then equal to $1 - P_{safe}$. The integral in (3) is evaluated using a Monte Carlo method.

The metric (3) essentially aims to compare the distributions of peaks under normal vibrations and under SIV. While it can be argued that standard metrics obtained from statistical tests like the χ^2 test or metrics that measure the distance between distributions like the Kullback–Leibler distance can be used to check if the distributions are similar, these methods have some disadvantages. Statistical tests have a high sensitivity (have a high power) when many data points are used to fit f_N, which is the case here and start detecting even slight deviations from f_N. Further, the statistical test and distance based methods require specification of a threshold to flag deviation from normal peaks. This introduces arbitrariness and reduces the robustness of the detection process. In contrast, the metric (3) gives a more relatable measure about the occurrence of SIV that is easier to use in decision-making.

2.2. MM state estimator method

2.2.1. The multiple model state estimation problem

Many real systems exhibit time varying behaviour meaning that there are different models describing the system behaviour at different times. The multi-model state estimation is used to identify the model that best describes the system at the current instant, and identify changes in the system behaviour while estimating the system states and model parameters. Given that the system is described by any one of the M models $\{m^1, m^2, ..., m^M\}$ at any time instant, the multi-model state estimation problem is formulated as:

Given measurements at time k and the initial values :

$$Y_k \triangleq y_0, y_1, y_2 \dots y_k \tag{4}$$

$$x_0 \in \mathrm{N}\left(\hat{x}_0, P_0\right), \left\{\mathrm{P}\left(m_0^j\right)\right\}_{j=1}^{M} \tag{5}$$

where x_0 is the initial state vector and $\left\{\mathrm{P}\left(m_0^j\right)\right\}_{j=1}^{M}$ is the probability density of the models at the time instant 0, find at each time instant:
1) State estimate $\hat{x}_k$ which minimizes the mean square error $\mathrm{E}\left(\left(x_k - \hat{x}_k\right)^{\mathrm{T}} A \left(x_k - \hat{x}_k\right)\right), A \geq 0$, and
2) Estimates of the model probability densities $\left(\mathrm{P}\left(m_k^1 \mid Y_k\right), \quad \cdots \quad \mathrm{P}\left(m_k^M \mid Y_k\right)\right)^{\mathrm{T}}$.

Different algorithms exist for multi-model state estimation such as the Generalized Pseudo- Bayesian algorithms [15], and the Interacting Multiple Model (IMM) algorithm [9], which is used in this work.

2.2.2. Development of the model used for state estimation

The behaviour of a standstill wind turbine for different inflow conditions broadly falls into the following categories: At low yaw angles when SIV do not happen, it behaves as a linearly stable system, at higher yaw angles, when SIV happens it behaves as an unstable system with the possibility of a limit cycle. The corresponding blade root edgewise bending moments are shown in Fig. 2.

To detect SIV using the MM state estimator method, a model of a wind turbine blade that can describe both the stable and unstable behaviours of the turbine shown in Figure 2 is first developed. A deterministic setting is considered first, where a vibrating blade is modeled using an Ordinary Differential Equation (ODE). The ODE is later extended to a Stochastic Differential Equation (SDE) to effectively model the effects of the turbulent wind. SIV is assumed to excite only one of the blade modes. The mode with

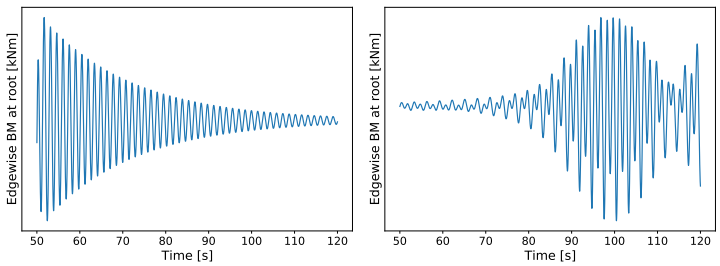

(a) *Linearly Stable.* **(b)** *Nonlinearly Unstable.*

Figure 2: Behaviour of a wind turbine for different inflow conditions. The latter is the characteristic of SIV.

undamped natural frequency ω_o and structural damping ρ of a clamped blade can be described by the ODE (6) where $z(t)$ is the blade position, $\dot{z}(t)$ is the blade speed, and $f_f(t)$ is the forcing term.

$$\ddot{z}(t) + 2\rho\omega_o\dot{z}(t) + \omega^2 z(t) = f_f(t) \tag{6}$$

A forcing term of the type $(\alpha + \beta u_\gamma(\dot{z}(t)))v(t)^2$ is proposed, where $v(t)$ represents the wind speed, α, β and γ are parameters and u_γ is the soft Heaviside step function defined as $u_\gamma(z) \triangleq \frac{1}{2}(1+\tanh(p(x-\gamma))$. p is a coefficient that influences the activation of the $\tanh$ function. The motivation for using this forcing term is to let the non-linear part of the forcing term, $\beta u_\gamma \dot{z}(t)v(t)^2$ to come into play when the yaw error is large ($\sim 30°$) with the same phase as $\dot{z}(t)$. Thus effectively, the proposed forcing term mimics the blade getting into stall at the extremes of vibration, and out of stall as it moves during the vibration, leading to growing vibrations. This type of forcing term was found to model the vibrations better than other forcing terms explored by the authors. Thus, (6) becomes

$$\ddot{z}(t) + 2\rho\omega\dot{z}(t) + \omega^2 z(t) = (\alpha + \beta u_\gamma(\dot{z}(t)))v(t)^2 \tag{7}$$

With a choice of state vector x as $x \triangleq [z \;\; \dot{z}]^T$, (7) can be written in the form $\dot{x}(t) = f(x(t), v(t), t)$, which is a classical technique. However, in such a formulation, the turbulent wind enters the equation as an input. To model the effect of the turbulent wind better, the wind model from [16] is adopted, in which the wind dynamics are modelled using an SDE with the wind speed included in the state vector and the turbulent part of the wind modelled with the noise corresponding to the wind speed state.

As per [16], the wind speed is split into an average component v_m and a turbulent component (fast moving) v_f. So, $v = v_m + v_f$. The blade movement is also split into an average component z_m and a varying component z_f (fast moving). So, $z = z_m + z_f$. This formulation was found to model the blade vibrations better. To simplify the derivatives, we assume that $\dot{z}$ is dominated by $\dot{z}_f$, and hence $\dot{z} \sim \dot{z_f}$.

v_m and z_m are modeled as Wiener processes and v_f is modeled as low pass filtered white noise. The differentials of v_f, v_m and z_m are then given by $dv_f = a(v_m)v_f dt + dw_1$, $dv_m = dw_2$, and $dz_m = dw_3$ where w_1, w_2 and w_3 are Weiner processes, and the definition of a is given in the following equations.

Collecting (7), and the definitions of z_m, z_f, v_m and v_f, an SDE of the form

$$dx(t) = f(x(t), t)dt + g(x(t), t)dw(t), \quad w(t) \in W(I), \tag{8}$$

where $W(I)$ is a Wiener process of the required size can be formulated with a 5-dimensional state vector x defined by $x \triangleq \left(v \;\; v_m \;\; z_f \;\; \dot{z} \;\; z_m\right)^T \triangleq (x_1 \;\; x_2 \;\; x_3 \;\; x_4 \;\; x_5)^T$ as

$$f(x,t) \triangleq \begin{pmatrix} a\left(x_2\right)\left(x_1 - x_2\right) \\ 0 \\ x_4 \\ -2\rho\omega x_4 - \omega^2\left(x_3 + x_5\right) + \left(\alpha + \beta u_\gamma\left(x_4\right)\right)x_1^2 \\ 0 \end{pmatrix}; \qquad g(x,t) \triangleq \begin{pmatrix} s\left(x_2\right) & 0 & 0 \\ 0 & s_m & 0 \\ 0 & 0 & 0 \\ 0 & 0 & 0 \\ 0 & 0 & s_b \end{pmatrix}$$

$$a\left(x_2\right) \triangleq -\frac{\pi x_2}{2L}, s\left(x_2\right) \triangleq \sqrt{\pi x_2^3 \sigma^2 L^{-1}}, s_m = \sqrt{5^2/600} \sim 0.20, s_b = s_m$$

(9)

where, σ is the turbulence intesity, and a value of 0.1 is assumed. L = 340.2 is the Integral length scale parameter of the turbulence model [16, 17]. The expressions for $a(x_2)$ and $s(x_2)$ are obtained by equating the variance and peak frequency of the turbulent wind to a Kaimal spectrum. s_m and s_b are obtained by assuming a wind speed variation of up to $5\,\mathrm{ms}^{-1}$ over a 10 minute period. The details of the derivation and the SDE formulation can be found in[16].

It can be seen that when β = 0, the model (9) represents a linear system with lightly damped vibrations and when $\beta > 0$, it represents a non-linear system with growing vibrations and limit cycles. These models are denoted as $\mathcal{M}_1$ and $\mathcal{M}_2$ respectively.

Now that the system dynamics is modeled using (9), a measurement model is defined to complete the formulation of a state-space model which is used for the state estimation. An edgewise load sensor at the blade root is used as a proxy for measurement of the blade position. The nacelle anomemeter readings give the instantaneous wind speed measurements with a standard deviation of 1 m/s as the nacelle anemometers is a uncertain effective wind speed measurement. These are the only 2 measurements considered available. The measurement noise is described by the covariance matrix R. The measurement equation can then be described by (10).

$$\begin{aligned} &y\left(t_i\right) = Hx\left(t_i\right) + v\left(t_i\right), H = \begin{pmatrix} 0 & 0 & 1 & 0 & 1 \\ 1 & 0 & 0 & 0 & 0 \end{pmatrix}, \\ &v\left(t_i\right) \in \mathrm{NID}(\underline{0}, R), R_{11} = 0.1, R_{22} = 1, R_{12} = 0 \end{aligned} \tag{10}$$

where NID refers to Normally and Independently Distributed variables.

Combining (9) and (10), and the state space model can be written as

$$\begin{aligned} dx(t) &= f^j\left(x\left(t_i\right), t_i\right) dt + g\left(x\left(t_i\right), t_i\right) d\omega(t) \\ y(t_i) &= Hx(t_i) + v(t_i) \end{aligned} \tag{11}$$

(11) is a Continuous- Discrete representation where the system dynamics is represented by the continuous time SDE but the measurements are obtained in discrete time. $f^j = \{\mathcal{M}_1, \mathcal{M}_2\}$ is one out of the two models. The probability of $\mathcal{M}_1$ and $\mathcal{M}_2$ is evaluated at each instant using the IMM method. The IMM is essentially a M number of Kalman filters running in parallel and estimating the states. In this work, since the model (11) is non-linear, an Unscented Kalman Filter (UKF) is necessary. The Continuous-Discrete UKF developed in [18] is used for state estimation.

3. RESULTS

Data collected from a Vestas turbine which had experienced standstill conditions is used to compare the performance of the models. The data was collected in a measurement campaign during which the turbine was always in a standstill condition with the rotor brake on. The turbine was exposed to different inflow conditions, including ones that are conducive to SIV, but did not always experience SIV.

While ω_o and ρ were known from the blade properties, the other required model parameters α, β, γ and p were tuned manually, and the following values are used: $\alpha = -0.5$, $\beta = 0.02$, $\gamma = 5$, $p = 10$.

The probability of SIV obtained using both methods in a scenario where SIV develops, sustains, and decreases is shown in figure 3. It can be seen that both methods are able to detect the presence of SIV. The peak monitoring method detects the presence of SIV much earlier than the MM estimator method. This is because the MM method is based on the model of the turbine and the trend of vibrations has an effect on its detection output more than the level of vibrations. It can be seen that the trend of clearly growing SIV appears only around 900s, while the vibration levels have already gone beyond the normal levels around 400s. Meanwhile the MM estimator has the advantage that it is able to detect the

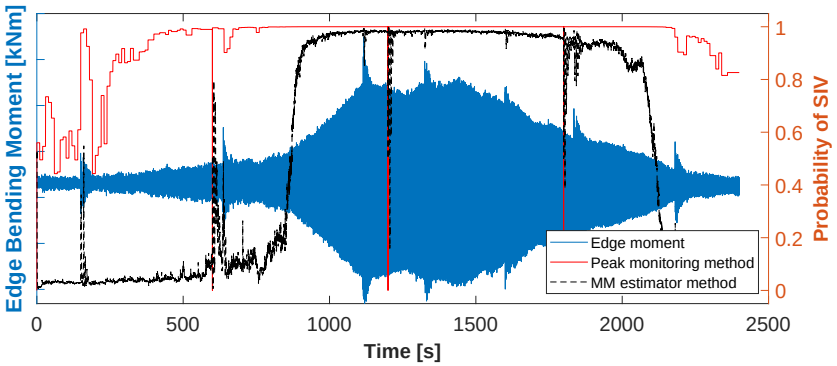

Figure 3: Detection of SIV using the different methods for a scenario with a clear growth, sustenance and decay of SIV.

beginning of reduction of SIV quicker, as clearly seen around 1800s. The peak monitoring method is solely based on the levels of vibrations and not the trend and requires that the vibration peaks have to reduce significantly before it gives a signal that SIV has attenuated. This feature of the MM estimator can be particularly useful in the context of deciding a control action to reduce the vibration amplitudes. Since the MM estimator gives a quicker feedback about the decreasing trend of SIV, the output of the MM estimator could be an added component to the objective function of the controller in addition to just the amplitude of vibrations, which takes a longer time to return to normal levels.

Further, the sensitive nature of the peak monitoring method can lead to false alarms in some cases. This is highlighted in figure 4 where we consider a scenario in which there is no SIV but just an increased level of vibrations due to the turbulent wind. The peak monitoring method flags a moderate to high level of probability of SIV based on the raised levels. However the MM method clearly does not detect any SIV as the vibrations do not have characteristics of SIV such as growth or sustained limit cycles. In this way, the MM estimator method is more robust.

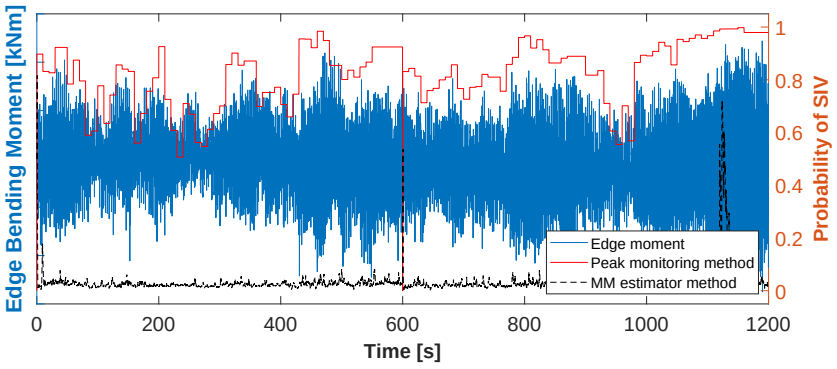

Figure 4: Detection of SIV using the different methods in a case where there is no SIV but just a higher than normal level of vibrations due to turbulence.

4. CONCLUSION

In this study, two different methods of detection of SIV are discussed. First, a simpler method based on monitoring the peaks of the vibrations is proposed. This method is based on establishing normal vibration levels collected from experiments or simulations and then checking for deviations from the normal levels. In this method, we have also introduced a metric that effectively describes the deviation of real time peaks from normal vibration levels. Next, a model based method is proposed, which is based on the multi model state estimation technique. A model of the vibrating blade is developed that

can cover both linearly lightly damped vibrations and non-linearly growing vibrations that transition into a limit cycle. Then, using the IMM state estimation technique, the probability of non-linearly growing vibrations is evaluated.

The results show that both the methods capture the presence of strong vibrations well. Simpler detection methods that are just based on metrics obtained from time-domain statistics of the vibrations, such as the peaks of the vibrations considered here used to detect SIV quickly. However, such methods cannot distinguish between growing and attenuating vibrations. On the other hand, model based detection methods, like the MM estimator method proposed here might have a slightly delayed detection but can also provide information about the decreasing trend of vibrations. This can be useful in devising control strategies.

This study is expected to serve as the basis for new studies to develop sophisticated models to detect SIV based on different control objectives and increase the safety of wind turbines in standstill turbines.

- Extension of the model based methods to include more characteristics of the model such as additional standstill rotor modes.
- Development of a yaw control algorithm to control SIV that takes into account the vibrations in addition to the yaw angle sensor measurements.

ACKNOWLEDGEMENTS

This research has been supported by Innovation Fund Denmark (grant no. 9090-00025B). The data from the measurement campaigns was provided by Vestas Wind Systems A/S.

REFERENCES

[1] Earl H Dowell. *A Modern Course in Aeroelasticity*. Springer, 4 edition, 2015.

[2] Morten H Hansen. Aeroelastic instability problems for wind turbines. *Wind Energy: An International Journal for Progress and Applications in Wind Power Conversion Technology*, 10(6):551–577, 2007.

[3] Witold Skrzypiński and Mac Gaunaa. Wind turbine blade vibration at standstill conditions-the effect of imposing lag on the aerodynamic response of an elastically mounted airfoil. *Wind Energy*, 18(3):515–527, 2014.

[4] PRESTIGE: Stability of wind turbines in standstill conditions. `https://wind.dtu.dk/projects/research-projects/prestige`, 2020 - 2023. Accessed: 2023-12-29.

[5] Christian Gjerløv, Imad Abdallah, and Brian Jørgensen. Wind turbine stand still load reduction. US Patent 8749084, 2014.

[6] H et al. Andreas. System and method for mitigating vortex-shedding vibrations or stall-induced vibrations on rotor blade of a wind turbine during standstill. US Patent US20210079896A1, 2021.

[7] Junda Zhu and Tom Nostrand et al. Survey of condition indicators for condition monitoring systems. In *Annual Conference of the PHM Society*, 2014.

[8] Chandramouli Santhanam, Riccardo Riva, and Torben Knudsen. Surrogate models for predicting stall-induced vibrations on wind turbine blades. In *Journal of physics: Conference series*, volume 2265, page 032005. IOP Publishing, 2022.

[9] Henk AP Blom and Yaakov Bar-Shalom. The interacting multiple model algorithm for systems with markovian switching coefficients. *IEEE Transactions on Automatic Control*, 33(8):780–783, 1988.

[10] Masoud Vaezi and Afshin Izadian. Multiple-model adaptive estimation of a hydraulic wind power system. In *39th Annual Conference of the IEEE Industrial Electronics Society*, 2013.

[11] Wai Hou Lio and Fanzhong Meng. Kalman-based interacting multiple-model wind speed estimator for wind turbines. *IFAC-PapersOnLine*, 53(2):12644–12649, 2020.

[12] David John Laino and Marcos Paulo Halal Lombardi. Controlling a wind turbine to reduce vibrations associated with collective rotor blade deflection in a standstill mode. DK Patent DK2024050049, 2024.

[13] Joel Igba and Kazem Alemzadeh et al. Analysing rms and peak values of vibration signals for condition monitoring of wind turbine gearboxes. *Renewable Energy*, 91:90–106, 2016.

[14] Robert E. Melchers and André T. Beck. The basic reliability problem. In *Structural Reliability Analysis and Prediction*, chapter 1, pages 14–16. John Wiley & Sons, 2018.

[15] Yaakov Bar-Shalom and Thomas E. Fortmann. *Tracking and Data Association*. Academic Press, 1988. ISBN 978-0120797603. Chapter 6 discusses the GPB algorithm.

[16] Torben Knudsen, Mohsen Soltani, and Thomas Bak. Prediction models for wind speed at turbine locations in a wind farm. *Wind Energy*, 14:877–894, 2011.

[17] International Electrotechnical Commission. 61400-1 cd iec:2014(e) draft. Technical report, IEC, 2014.

[18] Torben Knudsen and John Leth. A new continuous discrete unscented kalman filter. *IEEE Transactions on Automatic Control*, 64(5):2198–2205, 2018.